



Underwater Image Enhancement Using Deep Learning

Mr.S.Balaji ^{a*}, J.Vengatesan ^b, S.Satheesh kumar ^b, K.Egambaram^b

^a Assistant Professor, Department of CSE, Manakula Vinayagar Institute of Technology, Puducherry;

^b UG Student, Manakula Vinayagar Institute of Technology, Puducherry.

Abstract: The study of searching the ocean floor for both living things and non-living things is known as underwater archaeology. These kinds of studies are only achievable using sonar technologies. Sound is used as a source by the SONAR (SOund Navigation and Ranging) technology to create acoustic images of objects under the surface. Sonar comes in a variety of forms, and side scan sonar is one of the most accessible methods for visualising the bottom. The side scan sonar photos that are taken are frequently noisy, low contrast, and of poor visual quality. The acoustic images are displayed as grey scale images with different light and dark contrasts. This project's objective is to develop original picture-enhancing algorithms for object recognition in acoustic underwater images. The algorithms for image improvement include edge-preserving interpolation, intensity enhancement, contrast enhancement, and noise removal or denoising for object detection in audio pictures. Edgetech 4125 side scan sonar was employed in this research project to obtain the sound images. These images are affected by the speckle noise of the device. "SONAR" is an acronym for "Sound Navigation and Ranging." Sonar uses echoes to find and locate items beneath the sea, much to how porpoises and other marine animals do with their natural sonar systems. The suggested denoising method used Stationary Wavelet Transform and its shrinkage function to eliminate the speckle noises from the photos. Image enhancing methods were applied to the denoised photos. Two approaches based on multiresolution techniques were suggested. The Gaussian and Laplacian pyramid is used for intensity enhancement in the first enhancement technique. The second technique enhances the contrast of the photos using a Stationary Wavelet Transform and filtering methods. The suggested edge-based vi interpolation technique uses the improved image as input to increase the spatial resolution or size of the output images. Edge-based segmentation and object tracing algorithms are developed for the purpose of detecting objects in underwater sound pictures.

Index Terms—Deep learning, image processing, underwater, enhancement.

1.1 INTRODUCTION

Geo-technical, geophysical, and oceanographic studies are a result of the examination and use of the living and non-living undersea resources along the Indian coast. Because the sound wave may only travel a greater distance without noticeably weakening in the ocean, all of these research are only possible with the use of underwater acoustics or hydro acoustics based devices. In water, where light attenuates over shorter distances, signals are produced by sound and transformed into two-dimensional pictures. Today's acoustic devices can quickly map or photograph the ocean floor, examine below the surface of the water, and measure numerous oceanographic physical characteristics. extremely high level of accuracy and comparatively excellent resolving power. The word "SONAR" is an acronym for "Sound Navigation and Ranging." Sonar uses echoes to find and identify objects under the water, much like how porpoises and other marine animals use their innate sonar systems to navigate. Active sonar and passive sonar are the two types of sonar technology that are now accessible. An active sonar hears the echo of the pings (sound pulses) it has just sent out. Without sending out its own sound signals, passive sonar picks up sound echoes. When compared to regular sounds, the sound impulses used in active sonar are extremely potent. The majority of sonar emits noises that are a million times louder than a shout. Each ping lasts for a split second. Some sonar systems produce audible sounds. The human ear cannot hear some sonar waves because of their high pitch. Ultrasonic waves are the name for these transmissions. ("Ultra" denotes

"beyond," and "sonic" denotes "sound"). The sonar instrument has a special receiver that can pick up returning echoes. The position of submerged objects can then be determined using the time interval between sending the signal and receiving the echo back. Nowadays, it has been discovered that acoustic cameras, interferometric sonar, synthetic aperture sonar, synthesis incoherent sonar, parametric sonar, side scan sonar, etc. are used to gather underwater imagery. Modern side scan sonar is a great tool for conducting high-quality surveys of the seabed and is frequently used for underwater imaging among the diversity of sensors (Dura 2011). The sonar array creates sound waves in the form of fans that are perpendicular to the device's travel direction. Side scan sonar typically uses sound frequencies between 100 and 500 KHz. The image on the top processing unit will be created using the backscattered signals from each ping on the port (Reed et al. 2003). The sonar sends high frequency sound pulses into the water, where they interact with the objects. The programme receives the reflected waves and uses them to turn the return pulses into pictures. Images are created based on the object's distance and the volume of the echoes. The main variables that impact image quality include transmission loss, absorption, and scattering. Temperature, salinity, and sea level pressure are other elements that contribute to noisy and low contrast auditory pictures. Military, ecological, seismic, equipment monitoring, leak detection, and assistance for swarms of underwater robots are just a few of the uses for underwater acoustics

The sonar sends high frequency sound pulses into the water, where they interact with the objects. The programme receives the reflected waves and uses them to turn the return pulses into pictures. Images are created based on the object's distance and the volume of the echoes. The main variables that impact image quality include transmission loss, absorption, and scattering. Temperature, salinity, and sea level pressure are other elements that contribute to noisy and low contrast auditory pictures. Military, ecological, seismic, equipment monitoring, leak detection, and assistance for swarms of underwater robots are just a few of the uses for underwater acoustics.. There are aphotic or midnight zones below 1000 metres of water. Since sunlight can't penetrate thus far down, the area is completely dark. Manned and unmanned underwater vehicles are the two sorts of vehicles that can capture the ocean's scene. Remotely Operated Vehicles (ROV) and Autonomous Underwater Vehicles (AUV) are examples of unmanned underwater vehicles. AUVs are autonomous and can be controlled remotely from the surface, a ship, or land, whereas ROVs can be dragged by a boat from the surface at a moderate speed. Sonar is a tool that submarines use to find other ships. Using a tool called a fathometer, sonar is also used to gauge the depth of the water (one fathom equals 6 feet, or roughly 1.8 metres). The Fathometer determines how long it takes for a sound pulse to leave the ship and return to the bottom of the ocean. Fathometers are used by fishing vessels to locate fish schools. Oceanographers utilise sonar to map the topography of the ocean floor. Additionally, sound waves can be transmitted into the sand or mud on the ocean floor and hit a layer of rock beneath it. The distance to the rock stratum is then revealed by an echo that follows. When looking for oil on land, the same approach is used. A sonar pulse is sent into the ground. By listening for the echoes that return from the various layers of rock and soil, geologists can identify the different types of soils and rocks that are there. This helps them select drilling sites in areas where there is a high likelihood of finding oil or gas. Seismic 4 exploration is the name given to this underground mapping. Ultrasonography, often known as echoscopy, is a specific type of sonar utilised in medicine. High-frequency sound waves produce distinctive echoes when they are reflected by the body's organs. Doctors may utilise these echoes to detect disease and monitor the growth of an unborn child. Extremely high-frequency sound waves are used in both commerce and medicine to clean a range of materials by shaking loose minute dirt or other particles.

2.LITERATURE SURVEY

[1] The Herr wavelet transform (HWT), developed by Xie Kai and Li Tong, can distinguish between different sorts of edges, restore sharpness from the blurred version, and then determine whether or not a picture is blurry and how much, if at all. To estimate the movement blur parameters, two original approaches are suggested. The direction of the blur has been determined using a two-dimensional Gabor filter. The length of the blur has been determined using a radial basis function neural network (RBFNN).

Finally, the images have been corrected using the Wiener filter out. The suggested scheme's noise robustness is tested using specific noise strengths. The blur parameter estimation problem is tackled using a support vector machine (SVM) and is modelled as a sample category problem.[2] R.Dash, P. K. SA, and B. Majhi have introduced approach to estimate the motion blur parameters using Gabor filter for blur direction and radial basis function for blur length with sum of Fourier coefficients as features. Restoration attempts to recover an image by modeling the degradation function and applying the inverse process. motion blur is a commonplace type of degradation that is due to the relative motion among an object and digital camera. motion blur may be represented by a factor spread characteristic made up of the two variables perspective and duration. When blindly repairing motion-blurred snapshots, an accurate estimation of those characteristics is required. The methods used in this research to estimate the direction and length of a motion blur directly from a location-based image with and without the influence of Gaussian noise are contrasted. Once a typical non-blind de-convolution technique has been developed, these anticipated motion blur parameters can be used. [3] Blurred images for atmospheric turbulence have been introduced by Li and Simske. They made use of the idea that the amount of blurring affects the kurtosis of an image. It has been used to examine how blurring affects kurtosis in section shape. After putting the hunt region through trial and error, the blur parameter is estimated. Using a traditional image healing technique, the image is de-blurred for each of the predicted parameters.[4] Haiyong Liao, Fang Li, and Michael K have developed a quick image restoration technique that restores noisy blurred images by automatically choosing the regularisation value. To determine the amount of regularisation used in each restoration step, the technique takes advantage of the generalised pass validation approach. Every repetition, the regularisation parameter is updated, bringing the restored image's distance from the original shot closer.[5] In their capstan analysis, F. Kraemer, Y. Lin, B. McAdoo, K. Ott, J. Wang, D. Widemann, and B. Wohlberg concentrated on the Radon transform to look for motion blur features. The methods for assessing linear movement blur are covered in this report. The distorted image is modelled as a convolution of the real image and an unidentified factor-unfold.

4.METHODOLOGY

This chapter presents a shrinkage-based method for underwater acoustic picture denoising. The threshold selection in this suggested method uses Visushrink and Sureshrink approaches. The approach is contrasted with already-used filtering strategies such the directed, Wiener, Lee, bilateral, and median filters.

4.1 INTRODUCTION

Sensors that transmit and collect sound in the form of echoes make up side scan sonar. Surplus speckle noise that is created during the acquisition and transmission of the images is included in the images created using the echoes. The speckle noise reduces the clarity of the images produced by the active sonar. Brighter areas of the image are severely affected by the speckle noise, which also exhibits signal-dependent features. Filtering methods are employed to convert a black and white section of the sonar image to a smooth grey scale.

4.2 SPECKLE NOISE

Images produced by side scan sonar are impacted by speckle noise, a common disturbance. "Speckle" noise in coherent imaging systems results from either constructive or destructive interference. Its multiplicative nature means that it is closely correlated with the local grey level in the region. The relationship between the signal and noise is not linear. Statistics show that Speckle is unrelated to the local data. It is challenging to get rid of the multiplicative noise since it changes with the image intensity. In Equation (3.1), the general form of the speckle noise is shown.

$$y(i, j) = x(i, j)n(i, j) + a(i, j)$$

If $n(i, j)$ and $a(i, j)$ represent the multiplicative and additive noise, respectively, and $y(i, j)$ is the noisy

image, $x(i,j)$ is the original image. The speckle may also have information that can be utilised to gauge the surface's activity using the speckle pattern. In a picture, speckle is not noise, but rather noise in the form of contrast variation. When a sound wave pulse randomly interferes with tiny particles or things at a scale corresponding to the sound wavelength, the interference happens.

4.3 FILTERING TECHNIQUES FOR IMAGE DENOISING

The primary goal of the filtering process is to reduce image noise. Any noise reduction technique's goal is to eliminate all noise while preserving the images' key details.

4.4.1 Median Filter

According to Gonzalez and Woods (2007), median filters are frequently employed to reduce noise while maintaining the edges. When half of a set of values are less than or equal to m and the other half are more than or equal to m , the set of values has a median m . To get the neighborhood's median, the values in the filter are sorted. The resulting image is given the median value. A median filter's goal is to make points of varying brightness more similar to surrounding pixels. All of the image's pixels had the median filter applied consistently. As a result, it is employed to denoise the image at the expense of deformed features and excessive smoothing of the image's tiny details.

The median filter's instructions are provided by,

- A kernel can be created and centred around the pixel (i, j) in any centrally symmetric shape, such as a round disc, square, or rectangle, and in any size.
- The region's pixel intensity values are arranged in ascending order.
- The new value for pixel (i, j) is chosen to be the midway value.

4.4.2 Wiener Filter

The statistical method used by the Wiener filter (Gonzalez & Woods. 2007) is used to remove the noise from the image. By making the best feasible trade-off between noise smoothing and inverse filtering, the blurring and additive noise in the image are eliminated. They operate in the frequency domain, which makes them relatively sluggish. Given in Equation (3.2) is the Wiener filter.

$$f(u, v) = \left[\frac{H(u,v)^*}{H(u,v)^2 + \left[\frac{S_n(u,v)}{S_f(u,v)} \right]} \right] G(u, v)$$

- where the degradation function $H(u,v)$ is represented.
- As its complex conjugate, $H(u,v)^*$
- $G(u,v)$ depicts a deteriorated image.
- The noise power spectrum is represented by $S_n(u,v)$.
- The power spectra of the original image are shown by $S_f(u,v)$.

4.4.3 Lee Filter

Speckle noise data with an intensity related to the visual scene and an additive and/or multiplicative component are smoothed using Lee filters (Gonzalez & Woods, 2007). Lee filtering, a standard deviation-based (σ) filter, filters data in accordance with statistics calculated inside particular filter windows. In place of the pixel that is being filtered, a value calculated from the pixels nearby is used. Additionally, it uses MMSE to filter the image since it believes that speckle noise is distributed equally throughout all regions. As a result, it is inappropriate for images with sharp pixel changes, such as those near the edges. The edges become fuzzier as a result. Equation (3.3) provides the Lee filter.

4.4 Bilateral Filter

The technique used by the bilateral filter makes advantage of both the separation between pixels and the fluctuations in image intensity. In contrast to other filters, it combines the domain filter and the range filter. It is the result of the domain filter and the range filter mathematically. Therefore, smoothing doesn't happen if one of the weights is near to zero. The image might be divided into two parts, the filtered image and the residual image. The filter's filtered features or noise are seen in the remaining image. It is a fairly expensive algorithm despite being more edge-preserving. S and R are two parameters that influence it. Given the parameter range 40 The bilateral filter eventually approaches Gaussian convolution as r grows. Larger features are smoothed as the spatial parameter is increased. Equation (3.5) specifies the bilateral filter.

$$BF[I]_p = \frac{1}{W_p} \sum_{q \in S} G_{\sigma_s}(\|p - q\|) G_{\sigma_r}(\|I_p - I_q\|) I_q \quad (3.5)$$

$$\text{where } W_p = \sum_{q \in S} G_{\sigma_s}(\|p - q\|) G_{\sigma_r}(\|I_p - I_q\|) \quad (3.6)$$

The image value at pixel position p is represented by I_p , the set of all possible image locations is represented by S , the distance in Euclidean terms between pixels p and q is represented by q , the spatial Gaussian is represented by, the range Gaussian is represented by, and the normalisation factor is represented by W_p , which is represented by Equation (3.6).

4.4.5 Guided Filter

The guided filter employs a reference image known as the guiding image to reduce noise in the captured image. The input itself or another image may be used as the guide image. When another image is used as guide, the original image has the guidance image's features added to it. It is more edge-preserving and removes speckle noise when self-guided is used, which uses the same input as the guided image. It has numerous uses, including haze reduction, joint up sampling, image matting and feathering, detail enhancement, and HDR compression. For both grayscale and colour photos, the time complexity is $O(N)$, where N is the quantity of test photographs taken. The following equations (3.7) through (3.10) provide a guided filter.

$$q_i = a_k I_i + b_k \quad \forall i \in \omega_k \quad (3.7)$$

$$a_k = \frac{\frac{1}{|\omega|} \sum_{i \in \omega_k} I_i p_i - \mu_k \bar{p}_k}{\sigma_k^2 + \epsilon} \quad (3.8)$$

$$b_k = \bar{p}_k - \mu_k a_k \quad (3.9)$$

$$\bar{p}_k = \frac{1}{|\omega|} \quad (3.10)$$

where the linear coefficients (a_k, b_k) are thought to be constant in k . ω_k denotes the window centred at pixel k , μ_k represents the image's mean, and σ_k^2 represents its variance.

4.4.6 Homomorphic Filter

One technique for removing multiplicative noise is homomorphic filtering (Gonzalez & Woods, 2007). Since speckle noise is a multiplicative noise, it can be eliminated using a homomorphic filter. It is employed to fix uneven lighting in pictures. The intensity at any pixel, which is the quantity of light reflected by a point on the object, is determined by the illumination of the scene and the reflectance of the object(s) in the picture, as given by Equation (3.11) in the illumination-reflectance model of image

creation.

$$m(x, y) = i(x, y) \cdot r(x, y) \quad (3.11)$$

Here, the image is denoted by $m(x,y)$, the illumination by $i(x,y)$, and the reflectance by $r(x,y)$. Unlike reflectance, which can swiftly change at object borders, illumination typically changes gradually throughout the image. This discrepancy determines the capacity to discriminate between the light component and the reflectance component. The log function is used in homomorphic filtering to convert multiplicative components into additive components.

3.4 WAVELET BASED DENOISING PROCESS

A multiplicative granular noise known as "speckle noise" is brought on by erratic variations in the return acoustic signal. Given that it originates from several far separated targets, the image is affected. Continuous streams of signal and frequent individual noise speckles are seen in acoustic bearing displays. The device used to capture the pictures is the only reason why there are sounds in the acoustic images. Due to interference from the returning wave at the sonar transducer, there is speckle noise. For noise removal, these impacted photos should either be smoothed or denoised. Denoising reduces high frequency features like edges while retaining low frequency ones; smoothing does not. Contrarily, denoising eliminates noise independent of the signal's frequency composition. The wavelet-based denoising approach has shown to be one of the most effective denoising strategies. The steps of wavelet-based denoising are shown in Figure 3.1 and are as follows.

- Use SWT to decompose the picture.
- Use wavelet coefficient shrinkage denoising methods.
- Image reconstruction that keeps low frequency elements and uses Inverse SWT components like edges.

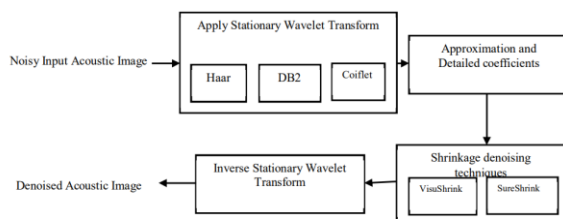


Figure 3.1: Steps in wavelet based denoising process

4.5 STATIONARY WAVELET TRANSFORM

Wavelet functions well for image denoising due to characteristics like sparsity and multiresolution structure. By applying wavelet basis, the transients and singularities may be represented as sparse piecewise regular one-dimensional signals. Large wavelet coefficients can be found in the edges and erratic textures of two-dimensional pictures. Wavelets can be categorised as continuous, discrete, stationary, multiwavelet, etc. based on their functions. While the discrete wavelet transform (DWT) is used for 2D pictures to collect frequency and position information, the continuous wavelet exclusively works with 1D signals. DWT lacks the translation invariant characteristic, despite the fact that many picture applications benefit from its use. Using DWT, the pictures are divided into low- and high-frequency components. These parts are just half as long as the original picture. Upsamplers are utilised in the synthesis phase, whereas downsamplers and filters are employed to create the frequency components during the analysis phase. By eliminating the downsamplers and upsamplers in the DWT, the Stationary wavelet transform (SWT) was created to get around the translation invariant characteristic. The redundant technique is employed to keep the image's length constant. Detailed coefficients and undecimated Noisy Input Acoustic Image Approximation are additional names for it. methods for shrinkage denoising inverse denoised acoustic image Wavelet Transform in Stationary Mode Utilise the stationary wavelet transform for the Haar DB2 Coiflet VisuShrink SureShrink 44. In SWT, the initial step is to apply At each level, apply high and low pass filters to the image. The

components that result are not decimated. The filters are then changed by padding zeroes at each level. The image's breakdown into low frequency and high frequency subbands is shown in Figure 3.2. LHi, HLi, and HH_i stand in for high frequency detailed edge characteristics of an image, while i=1, 2... stands for the levels of decomposition. LL_i stands for the low frequency smooth area in the picture.



Figure 3.2 First and Second level decomposition of image using SWT

In this work, the acoustic picture is broken up into three separate wavelet types—Haar, Daubechies, and Coiflet—and their inverses are utilised to rebuild the denoised image (Singh & Shiv Raj, 2014).

4.5.1 Daubechies Wavelet

Although the Haar transform may dissect a picture easily, it does not give the necessary smoothness. The Daubechies wavelet family was introduced and is characterised by a maximum number of vanishing moments in order to integrate the necessary smoothness. It is a well-liked orthogonal wavelet for analysing texture features. All variations in pixel intensity are reflected because the Daubechies wavelet uses overlapping windows rather than nearby pixel values. The Daubechies D4 transform uses four wavelet and scaling coefficients. Since the sum of the scaling function coefficients is also 1, the calculation averages four adjacent pixels. Daubechies averages across more pixels to get the smoothness needed for noise reduction.

4.5.3 Coiflet Wavelet

Coiflets are comparable to Daubechies wavelets, with the exception that they employ six wavelet function coefficients for scaling. The overlapping is more likely to be significant as the number of function coefficients rises. More smoothing results as a result of increased pixel averaging and differencing. They perform well for texture image denoising.

4.6 THRESHOLDING TECHNIQUES

Smoothing the pictures involves using a variety of linear and nonlinear spatial filtering techniques. These methods usually help to lessen the loudness. The size of the kernel being convolved with the picture determines how blurry and smooth the image will be. Although the filter size in the wavelet domain can be set, the image can still be seen in many resolutions. Thresholding, a straightforward nonlinear approach, is essential when working with wavelet coefficient. Either hard thresholding or soft thresholding can be used to choose the threshold.

4.6.1 Hard Threshold

The hard thresholding approach employs a rigid strategy in which coefficients are either left unchanged or set to zero. The threshold value is compared with the coefficients generated using the wavelet transform. If the coefficient falls below or is equal to the threshold, it is set to zero; otherwise, it is kept. Equation (3.16) depicts the hard thresholding DH and Co signifies the coefficient for a particular threshold T.

$$D^H(Co|T) = \begin{cases} 0 & \text{for } |Co| \leq T \\ Co & \text{for } |Co| > T \end{cases} \quad (3.16)$$

4.6.2 Soft Threshold

Hard thresholding techniques, which are based on pixel intensity, might be helpful in cases of spatial domain filtering. Hard thresholding is not desirable in the wavelet domain, where the coefficients are needed for picture denoising. The wavelet shrinkage technique, also known as soft thresholding, works

well for picture denoising in the wavelet domain. The wavelet coefficient is compared to the T value in this case, given the threshold T. if coefficient decreases or remains constant

4.7.1 Experimental Results

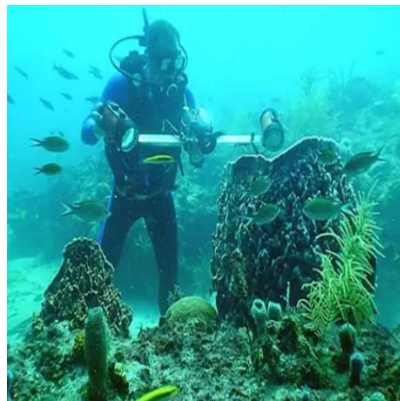


Figure 4.3 Original image.



Figure 4.4 Enhancement image

4.7.2 Performance Measures

Peak Signal to Noise Ratio (PSNR), Speckle Suppression Index (SSI), Speckle Image Statistical Analysis (SISA), Edge-Enhancing Index (EEI), and Feature-Preserving Index (FPI) are some objective metrics that are used to compare how well the proposed system works.

5. CONCLUSION AND FUTURE WORK

5.1 CONCLUSION

In this study, we created image enhancing methods for object recognition in underwater acoustic pictures. Edgetech 4125 side scan sonar was used to capture the collection of photos used for study. The photos were collected utilising a 4125 tow vehicle, a 4125 portable topside processor, and a tow wire with a 400–600 KHz frequency. In the Bay of Bengal, the sonar was submerged to a depth of 20 metres, and Edgetech's Discover software was used to record the scene of the ocean floor. For the purpose of detecting objects in acoustic pictures, the image enhancement techniques of image denoising, intensity enhancement, contrast enhancement, and interpolation were developed. The instrument's speckle noise often has an impact on the acoustic pictures. Because to the salinity, pressure, and sea floor sediments, they have a low contrast. Side scan sonar often produces poor resolution pictures where it is quite challenging to distinguish between the items. These factors made the need for acoustic image enhancing approaches necessary. With the help of the Stationary Wavelet Transform and its shrinkage function, the suggested denoising approach was able to eliminate a multiplicative speckle noise from the photos. First, SWT was used to separate the input picture into its low- and high-frequency components. For the approximate and precise coefficients, both the 126 Sureshrink functions and the Visushrink functions are used. The denoised image is recreated using the inverse SWT. By achieving the threshold while maintaining the information, this approach effectively removed the speckle. Performance indicators including PSNR, SSI, SISA, EEI, and FPI demonstrated an improvement in picture quality. Intensity and contrast enhancement were applied to the denoised picture. An method based on multiresolution was employed to increase the picture intensity. Using a Gaussian kernel, the pictures were divided into different levels, and a Gaussian pyramid was formed. The Gaussian pyramid was then used to build a Laplacian pyramid. After using filtering techniques such histogram equalisation and unsharp masking approaches, the improved picture was recreated. The PSNR measurement made it clear that the quality had improved. The low contrast denoised photos were again

enhanced with SWT and Laplacian filters. The masking approach is used to improve the low frequency components produced by SWT. The difference between the Laplacian filtered picture and the low frequency sub-band was used to produce a mask. Along with the low frequency component, this mask was introduced. Inverse SWT was used to rebuild the augmented picture. The identical procedure is applied again with DWT, and the outcomes are contrasted. The acoustic images' quality has increased, as seen by performance indicators like PSNR and SSIM. low quality pictures made it exceedingly challenging to distinguish the items in the auditory images. The spatial resolution, which is the size of the pictures, is indicated by the resolution in this case. An edge-preserving interpolation method was suggested in order to enlarge the photos. This approach takes into account the diagonal, horizontal, and vertical pixels independently. The availability of edges is determined by the 127 gradient of the pixels. This approach interpolated the unknown pixel values using these pixel values. The detection of items in the improved pictures is the ultimate goal of this study endeavour. Using the Wiener filter and morphological processes like dilation and erosion, an edge-based segmentation technique was presented. The Moore's object tracing technique uses the edges to find the items in the underwater picture.

5.2 RESEARCH CONTRIBUTIONS

We have provided novel picture enhancing methods for item recognition in underwater acoustic images to this research endeavour. The following are some of the research's contributions: • An effective speckle noise reduction method employing SWT and shrinkage functions like Visushrink and Sureshrink.

- A method for enhancing intensity that combines multiple-resolution-based Gaussian and Laplacian pyramid filters with unsharp masking and histogram equalisation.
- Two methods for enhancing contrast, one using DWT and the Laplacian filter and the other using SWT.
- Creating the high resolution image using an edge-preserving interpolation approach to display the items clearly.
- A Moore's boundary tracing approach is used after an edge-based segmentation method to locate the object's borders utilising Wiener and morphological processes.

5.3 FUTURE WORK

Future extensions of this study might include:

3D picture segmentation:

Due to its qualities and features, interpreting acoustic images is undoubtedly a more challenging task for a human operator. The gap between low level characteristics and high level symbolic features would be filled by the extraction of models from pictures. The extraction of regional elements such as surface normals, 3D edges, curvatures, etc. can serve as the foundation for 3D acoustic picture segmentation. Finding the characteristics in an auditory picture is difficult since they are particularly susceptible to noise. The development of 3D picture segmentation would require new methodologies to address these issues.

Underwater object recognition:

Preprocessing and segmentation techniques can be used to find objects in underwater audio pictures. However, object identification is a challenging problem that calls for machine learning techniques. For the training and testing phases of machine learning algorithms, enormous amounts of pictures are required. Techniques for classification can be employed if training data are available. If training data are unavailable, a method for object recognition that dynamically incorporates ambient factors into the processed sonar data might be suggested.

Tool for creating a 3D model of the underwater scene:

In both the real world and the realm of computer graphics, underwater sceneries are an intriguing setting to see. The 3D tool would be suggested for making a 3D model of the underwater scene, which entails building terrain models, surface models, and textures out of 3D points made from local characteristics.

6. REFERENCE

1. Adelson, EH, Anderson, CH, Bergen, JR, Burt, PJ & Ogden, JM, 1984, 'Pyramid methods in image processing', *RCA engineer*, vol. 29, no. 6, pp. 33-41.
2. Anbarjafari, G, Izadpanahi, S & Demirel, H 2015, 'Video resolution enhancement by using discrete and stationary wavelet transforms with illumination compensation', *Signal Image Video Processing*, vol. 9, no. 1, pp. 87-92
3. Andrew J Patti & Yucel Altunbasak 2001, 'Artifact Reduction for Set Theoretic Super Resolution Image Reconstruction with Edge Adaptive Constraints and Higher-Order Interpolants', *IEEE Transactions On Image Processing*, vol. 10, no. 1.
4. Anwar, S, Porikli, F & Huynh, CP 2017, 'Category-specific object image denoising', *IEEE Transactions on Image Processing*, vol. 26, no. 11, pp.5506-5518.
5. Arici, T, Dikbas, S & Altunbasak, Y 2009, 'A histogram modification framework and its application for image contrast enhancement', *IEEE Transactions on Image Processing*, vol. 18, no. 9, pp. 1921-1935.
6. Asmare, MH, Asirvadam, VS & Hani, AFM 2015, 'Image enhancement based on contourlet transform', *Signal Image Video Processing*, vol. 9, no. 7, pp. 1679-1690.
7. Beugeling, Trevor & Alexandra Branzan-Albu 2013, 'Detection of objects and their shadows from acoustic images of the sea floor', In *IEEE Oceans-San Diego*, pp. 1-5.
8. Bhandari, AK, Soni, V, Kumar, A & Singh, GK 2014, 'Artificial Bee Colony-based satellite image contrast and brightness enhancement technique using DWT-SVD', *International Journal of Remote Sensing*, vol. 35, no. 5, pp. 1601-1624.
9. Bhandari, AK, Kumar, A, Chaudhary, S & Singh, GK 2017, 'A new beta differential evolution algorithm for edge preserved colored satellite image enhancement', *Multidimensional Systems and Signal Processing*, vol. 28, no. 2, pp. 495-527. 131
10. Brahim, Naouraz, Didier Guériot, Sylvie Daniel & Basel Solaiman, 2011, '3D reconstruction of underwater scenes using DIDSON acoustic sonar image sequences through evolutionary algorithms', In *OCEANS, IEEE-Spain*, pp. 1-6.
11. Celik, Turgay & TardiTjahjadi, 2011, 'A novel method for sidescan sonar image segmentation', *IEEE Journal of Oceanic Engineering*, vol. 36, no. 2, pp. 186-194.
12. Chang, Yet-Chung, Shu-Kun Hsu & Ching-Hui Tsai, 2010, 'Sidescan sonar image processing: correcting brightness variation and patching gaps', *Journal of marine science and Technology*, vol. 18, no. 6, pp. 785-789.
13. Chen, MJ, Huang, CH & Lee, WL 2005, 'A fast edge-oriented algorithm for image interpolation', *Image and Vision Computing*, vol. 23, no. 9, pp. 791-798.
14. Chen, Ting, QH Wu, Reza Rahmani-Torkaman & Jim Hughes, 2002, 'A pseudo top-hat mathematical morphological approach to edge detection in dark regions', *Pattern Recognition*, vol. 35, no. 1, pp. 199-210.
15. Chen, ZY, Abidi, BR, Page, DL & Abidi, MA 2006, 'Gray-level grouping (GLG): An automatic method for optimized image contrast enhancement-part I: The basic method', *IEEE Transactions on Image Processing*, vol. 15, no. 8, pp. 2290-2302.
16. Chen, ZY, Abidi, BR, Page, DL & Abidi, MA 2006, 'Gray-level grouping (GLG): An automatic method

- for optimized image contrast enhancement-part II: The variations', *IEEE Transactions on Image Processing*, vol. 15, no. 8, pp. 2303-2314.
17. Cherifi, D, Beghdadi, A & Belbachir, AH 2010, 'Color contrast enhancement method using steerable pyramid transform', *Signal, Image and Video Processing*, vol. 4, no. 2, pp. 247-262. <https://doi.org/10.1007/s11760-009-0115-6>.
 18. Chiang John, Y, Ying-Ching Chen & Yung-Fu Chen, 2011, 'Underwater image enhancement: using wavelength compensation and image dehazing (WCID)', In *International Conference on Advanced Concepts for Intelligent Vision Systems*, pp. 372-383. Springer, Berlin, Heidelberg.
 19. Chi-Kun Lin, Yi-Hsien Wu, Jar-Ferr Yang & Bin-Da Liu 2015, 'An iterative enhanced super-resolution system with edge-dominated interpolation and adaptive enhancements', *EURASIP Journal on Advances in Signal Processing*.
 20. Chi-Shing & Wong Wan-Chi Siu, 2010, 'Adaptive Directional Window Selection For Edge-Directed Interpolation', *IEEE Computer Communications and Networks*.
 21. Chi-Shing Wong & Wan-Chi Siu, 2010, 'Further Improved EdgeDirected Interpolation And Fast EdI For Sdtv To Hdtv Conversion', *European Signal Processing Conference*.
 22. Cho, Hyeonwoo, JuhyunPyo, JeonghweGu, HangilJeo & Son-Cheol Yu, 2015, 'Real-time noise reduction for sonar video image using recursive filtering', In *OCEANS'15 MTS/IEEE Washington*, pp. 1-8.
 23. Chouhan, R, Pradeep Kumar, C, Kumar, R & Jha, RK 2012, 'Contrast enhancement of dark images using stochastic resonance in wavelet domain', *International Journal of Machine Learning and Computing*, vol. 2, no. 5, p. 711. <https://doi.org/10.7763/IJMLC.2012.V2.220>.
 24. Demirel, H, Anbarjafari, G & Jahromi MNS 2008, 'Image equalization based on singular value decomposition', In: *IEEE 23. rd International Symposium on Computer and Information Sciences, ISCIS'08*, (pp. 1-5)
 25. Demirel, H, Ozcinar, C & Anbarjafari, G 2010, 'Satellite image contrast enhancement using discrete wavelet transform and singular value decomposition', *IEEE Geoscience Remote Sensing Letter*, vol. 7, no. 2, pp. 333-337
 26. Dura, E 2011, 'Image processing techniques for the detection and classification of man made objects in sidescan sonar images, sonar systems', In: Nikolai K (ed) *INTECH*. <http://www.intechopen.com/books/sonar-systems/image-processingtechniques-for-the-detection-and-classification-of-man-madeobjectsin-side-scan-sonar>.
 27. Elaraby, AEA, Hassan Badry, M, Ahmed El-Owny, M, Heshmat, M Hassaballah & Abel Rardy, AS 2013, 'A Novel Algorithm for Edge Detection of Noisy Medical Images', *Journal of International Signal Processing, Image Processing, and Pattern Recognition*, vol. 6, no. 6: pp. 365-374. 133
 28. Erik Meijering, 2002, 'A Chronology of Interpolation: From Ancient Astronomy to Modern Signal and Image Processing', *Proceedings Of The IEEE*, vol. 90, no. 3.
 29. Fan, F, Ma, Y, Li, C, Mei, X, Huang, J & Ma, J 2017, 'Hyperspectral image denoising with superpixel segmentation and low-rank representation', *Information Sciences*, vol. 397, pp.48-68.
 30. Feng Ling, Giles M. Foody, Yong Ge, Xiaodong Li, & Yun Du 2016, 'An Iterative Interpolation Deconvolution Algorithm for Super resolution Land Cover Mapping', *IEEE Transactions On Geoscience And Remote Sensing*, vol. 54, no. 12.